Proceedings of the Twenty-seventh (2017) International Ocean and Polar Engineering Conference **www.isope.org**
San Francisco, CA, USA, June 25-30, 2017

ISBN 978-1-880653-97-5; ISSN 1098-6189

Experimental Validation of SPH for Wave Generation and Propagation in Large Wave Tank

Andi Trimulyono[a,b], Hirotada Hashimoto[a], Kouki Kawamura[c]
[a] Graduate School of Maritime Sciences, Kobe University
5-1-1, Fukae-minamimachi, Higashinada-ku, Kobe, Hyogo, Japan
[b] Department of Naval Architecture, Diponegoro University
Jalan Prof. Soedarto, SH Tembalang, Semarang, Indonesia
[c] National Maritime Research Institute
6-38-1, Shinkawa, Mitaka, Tokyo, Japan

ABSTRACT

Smoothed Particle Hydrodynamics (SPH) is a well-known particle method for computational fluid dynamics (CFD) base on Lagrangian framework. In the present paper we carried out systematic validation of a SPH model for wave generation and propagation problems. For this purpose, we conducted a series of wave-generation tests at a wave tank of Kobe University using a piston-type wave maker. A wave probe for measurement of wave elevation is set at far from the wave maker and a pressure sensor is also set at the same distance. The wave-generation test is repeated for three water depths and two periods of piston motion with three different strokes. In SPH simulation, the measured piston motion of the wave-making board is directly imposed and numerical results are compared with the experimental ones. Sophisticated validation of SPH for representation of wave generation and propagation is conducted through comparisons with the dedicated experiments in large wave basin. In addition, we carry out a similar comparison study on large-deformation of wave surface due to existence of box-shape obstacle in shallow water condition.

KEY WORDS: SPH, Wave generation and propagation, Large wave tank, Deep and shallow waves, Motion of wave maker, GPU.

NOMENCLATURE

c	Speed of sound
h	Smoothing length
m	Mass of particle
P	Pressure
$\boldsymbol{r}$	Particle position vector
$\boldsymbol{u}$	Particle velocity vector
W	Kernel function
$\boldsymbol{\Gamma}$	dissipative vector
Π_{ab}	artificial viscosity term
δ,α	Intensity of numerical corrections
ρ	fluid density

INTRODUCTION

Wave generation, propagation and deformation are important issues in naval architecture and ocean engineering. Therefore a lot of theoretical, experimental and numerical studies have been done. Representation of nonlinear waves is one of major problems in seakeeping, stability and maneuverability of ships because green water, slamming, propeller racing, capsizing and ship handling in adverse conditions are to be handled. Recently strongly nonlinear waves such as freak waves and tsunamis are highlighted because they could lead to serious accidents/disasters. Application of CFD is a straightforward way nowadays to deal with such nonlinear waves thanks to the rapid advancement of computer performance. Therefore CFD could be an alternative to physical experiments where a lot of restrictions/limitations exist, if sufficient computer resources are available to achieve the required accuracy.

In the present paper we try to reproduce wave generation and propagation in deep and shallow waters using SPH which is a well-known Lagrangian-based particle method. SPH was originally introduced for astrophysics application (Gingold and Monaghan, 1977) and was applied to free-surface flows (Monaghan, 1994). SPH has been used in many research fields dealing with nonlinear water waves such as interaction between a ship and nonlinear waves (Le Touzé et al, 2010; Kawamura et al, 2016) and coastal sea breakwater (Gotoh et al, 2004; Shao, S.D., 2005; Altomare et al., 2014) , These outcomes well demonstrate good applicability of SPH to fluid-structure interactions.

Although SPH has been applied to many water wave problems, validation studies on wave generation and propagation are limited to relatively short distance (e.g. Antuono et al., 2011; Barreiro et al., 2013; Skillen et al., 2013) and detailed discussion on dynamic wave pressure is quite limited. Therefore sophisticated validation on wave generation and propagation is needed based on comparison with experiments in a long wave tank before tackling realistic engineering problems. For this purpose a series of experiment for systematic validation of a SPH model is newly conducted at a wave basin of Kobe University. The wave generation test is repeated for three different water depths, covering deep to shallow waters, using a piston-type wave maker with three amplitudes and two periods for piston motion.

In the validation of SPH, wave generation, propagation and deformation are simulated by directly imposing the motion of wave-making board measured in the experiment. This validation is attempted to cover the range from deep to shallow water waves. As a result, the SPH simulation using sufficiently large number of particles reproduces physical features of water waves quantitatively, i.e. wave amplitude, waves surface profile, phase velocity, wave pressure around free

surface and large deformation of wave.

MODEL EXPERIMENT

A dedicated experiment for validation is conducted at a wave basin of Kobe University (see Fig.1), whose length is 60 m, width is 6 m and changeable water depth is from 0 to 1.5 m. We generate regular waves using a piston-type wave maker and water elevation of propagated waves is measured by a wave probe placed at 24.6 m distance from the front face of wave-making board. A pressure sensor is attached to the bottom of the wave basin to measure wave pressure at the same distance with the wave probe, as shown in Fig.1. A piston motion of the wave maker is directly measured by a laser distance sensor attached to a fixed frame in front of the wave-making board as in Fig.2. Therefore we can use the measured piston motion (real output) in numerical simulation of wave generation. In addition, wave surface profile is also recorded by a video camera, set at the same position of wave probe and pressure sensor, through an observation window. The validation study is made with use of these experimental data, i.e. time histories of piston motion including gradual start at beginning and of wave elevation measured at a position far from the wave maker, wave surface profile obtained as a video image, and pressure variation at the bottom of basin due to wave passage.

In the experiment, we use three amplitudes and two periods of piston motion for wave generation as presented in Table 1. Table 2 show water depths, ratio of water depth and wave length. Here wave length, λ, is calculated based on small wave amplitude assumption given as Eq.1. The condition of h=1.1 m and T=1.15 s is only a deep water case and the others are shallow water cases.

$$\lambda = \frac{gT^2}{2\pi}\tanh\left(\frac{2\pi h}{\lambda}\right) \tag{1}$$

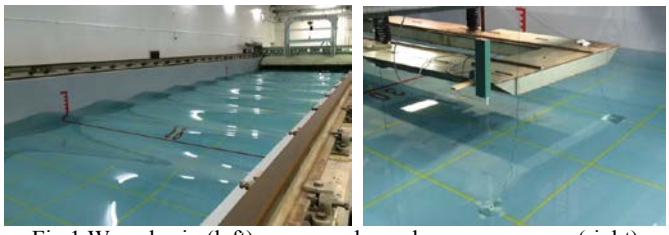

Fig.1 Wave basin (left), wave probe and pressure sensor (right)

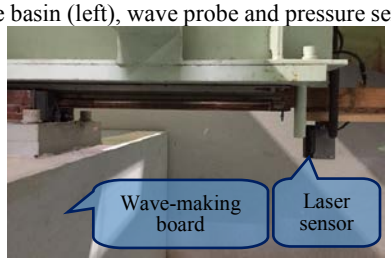

Fig.2 Setup for measurement of piston motion

Table 1 Period and amplitude of piston motion

Period: T (s)	
1.95	1.15
Amplitude: A (mm)	
16.5	16.5
33.0	33.0
50.5	50.5

Table 2 Water depth and h/λ ratio

Water depth: h (m)	T=1.95 (s) h/λ	T=1.15 (s) h/λ
1.1	0.21	0.53
0.75	0.16	0.37
0.4	0.11	0.22

Although input gain for the actuator of wave-maker board changes wave amplitude almost linearly, the input gain is carefully adjusted by trial and error to realize the same amplitude of piston motion for different water depths and wave periods. We also conducted a wave generation test with a box-shape obstacle placed in 24.6 m from the wave maker, with water depth of 0.6 m to capture wave surface deformation due to sudden change of water depth.

NUMERICAL SIMULATION

Smoothed Particle Hydrodynamics

SPH is a fully lagrangian mesh-less method. The technique discretizes a continuum using moving particle (evaluation points) and physical quantities (position, velocity, density and pressure) are computed as interpolation values of neighbouring particles. SPH was firstly derived for astrophysical field and is widely used to solve free surface flow problems represented by dam breaking.

Momentum equation is written as

$$\frac{d\boldsymbol{u}}{dt} = -\frac{\nabla P}{\rho} + \boldsymbol{g} + \boldsymbol{\Gamma} \tag{2}$$

In Lagrangian formalism

$$\frac{D\boldsymbol{r}}{Dt} = \boldsymbol{u}. \tag{3}$$

In standard SPH, liquids are treated as weakly compressible (WCSPH) and pressure field can be evaluated using Tait's equation

$$P = \frac{c_0^2\rho_0}{\gamma}\left[\left(\frac{\rho}{\rho_0}\right)^{\gamma} - 1\right], \tag{4},$$

where $\gamma = 7$, $\rho_0 = 1000$ kg/m^3 and $c_0 = c(\rho_0) = \sqrt{(\partial P/\partial\rho)|_{\rho 0}}$.

In this study, an open source SPH solver of DualSPHysics ver.4.0 is used. DualSPHysics is executed on CPUs using openMP or in GPU for parallelization to accelerate calculation speed for realizing large-scale particle simulation (Crespo et al., 2015). DualSPHysics can be downloaded at http://www.dual.sphysics.org. In DualSPHysics, artificial density diffusion (Molteni and Colagrossi, 2009; Marrone et al., 2011) as well as artificial viscosity (Monaghan, 1992) is introduced to the continuity equation and the momentum equation as a diffusive term to suppress numerical instabilities and high-frequency pressure fluctuation. Governing equations of δ-SPH formalism used in this study are expressed as follows

$$\frac{d\rho_a}{dt} = \sum_b m_b\boldsymbol{u}_{ab}\cdot\nabla_a W_{ab} + 2\delta_\varphi hc_0\sum_b\left(\rho_b - \rho_a\right)\frac{\boldsymbol{r}_{ab}\cdot\nabla_a W_{ab}}{\boldsymbol{r}_{ab}^2}\frac{m_b}{\rho_b} \tag{5}$$

$$\frac{d\boldsymbol{u}_a}{dt} = -\sum_b m_b\left(\frac{P_b + P_a}{\rho_b\cdot\rho_a} + \Pi_{ab}\right)\nabla_a W_{ab} + \boldsymbol{g} \tag{6}$$

$$\Pi_{ab} = \begin{cases} \dfrac{-\alpha \overline{c_{ab}} \mu_{ab}}{\overline{\rho_{ab}}} & \boldsymbol{u}_{ab} \cdot \boldsymbol{r}_{ab} < 0 \\ 0 & \boldsymbol{u}_{ab} \cdot \boldsymbol{r}_{ab} > 0 \end{cases} \quad (7)$$

where

$\mu_{ab} = h\boldsymbol{u}_{ab} \cdot \boldsymbol{r}_{ab} / (r_{ab}^2 + \eta^2)$, $\overline{c_{ab}} = 0.5(c_a + c_b)$, $\overline{\rho_{ab}} = 0.5(\rho_a + \rho_b)$, $\eta^2 = 0.01h^2$.

Numerical Domain

Schematic view of a numerical wave basin is presented in Fig.3. The dimension of wave basin, positions of wave probe, pressure sensor and box-shape obstacle are exactly same with the experiment. Parameters used in DualSPHysics are presented in Table 3. In SPH simulations, we generate regular waves by imposing the measured piston motion of wave-making board as the moving wall boundary. Parallel computing in DualSPHysics can be executed on GPU, so significant reduction of computation time can be achieved. Wave surface elevation and wave pressure is detected at the same position with the experiment.

All simulations are performed in 2-D because only single-directional waves are generated in the experiment. Particle size and total number of particles are given in Table 4. Constant particle size is used for all water depths.

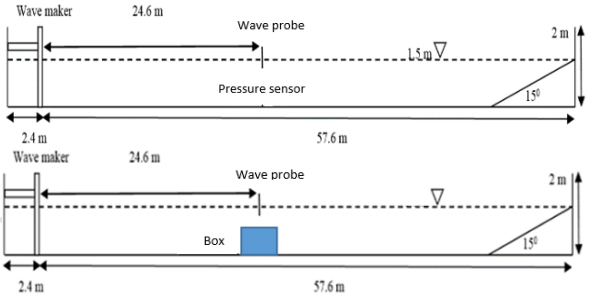

Fig.3 Schematic view of numerical wave basin w/ and w/o box

Table 3 Calculation condition

Kernel function	Wendland
Time step algorithm	Sympletic
Viscosity treatment	Artificial with α=0.0001
Coefsound	20.0
Particle size (mm)	3.0
Coefh	2.0
CFL number	0.3
Delta-SPH	0.1
Duration of simulation (s)	45.0

Table 4 Particle distance and total number of particles

Size of fluid particle (mm)	Water depth h (m)	Total number of particles
3.0	1.1	6,724,154
	0.75	4,521,922
	0.4	2,388,834

RESULTS AND DISCUSSION

Wave generation and propagation

SPH simulations are executed using single GeForce GTX TITAN X 12GB GDDR5. The computation time for water depth of 1.1 m (6.7 M articles) is about 65 hours for 50 seconds simulation including 5 seconds for settling down the fluid particles at beginning. Time histories of the measured piston motion can be found in Fig.4. These time histories are used as the input data for the piston motion in the SPH simulation. Figs.5-7 show comparisons of wave elevation between the experiment and simulation for T=1.95 s with three water depths from 0.4 to 1.1 m. The piston motion starts at t=0 s both in experiments and simulations. The SPH results show fairly good agreement with the experiment in developing rate, steady wave amplitude and wave celerity in shallow water. Certain average-shift of wave elevation can be found especially for smallest amplitude of piston motion at water depth of 0.4 m. This is because the wave amplitude is too small (10.3 mm) for the used particle size (3 mm). The number of particles in vertical direction is insufficient and the accuracy of wave reproduction becomes worse consequently. This presumption is supported by an additional simulation, using particle size of 2 mm, presented in Fig.8. Since the wave amplitude becomes small with the decrease of water depth in shallow water condition, required number of fluid particles changes even if the motion amplitude of wave maker is same.

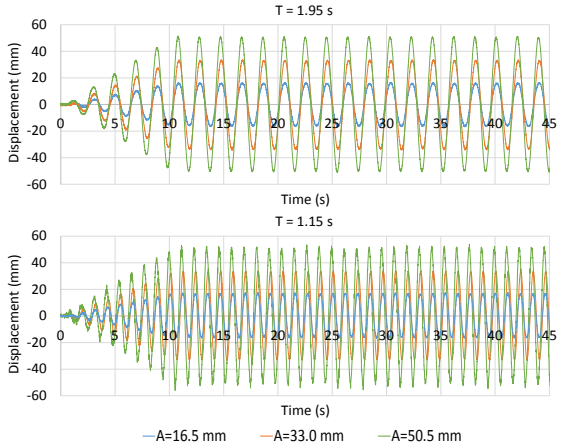

Fig.4 Measured time histories of displacement of wave-making board

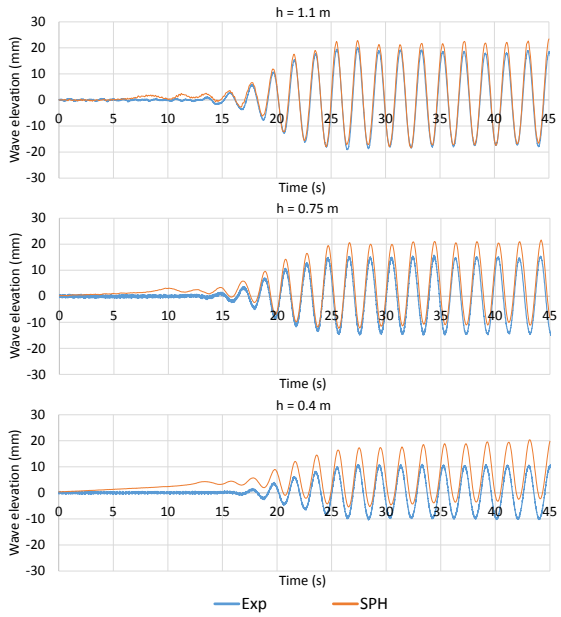

Fig.5 Comparison of wave elevation between experiment and SPH with A=16.5 mm and T =1.95 s

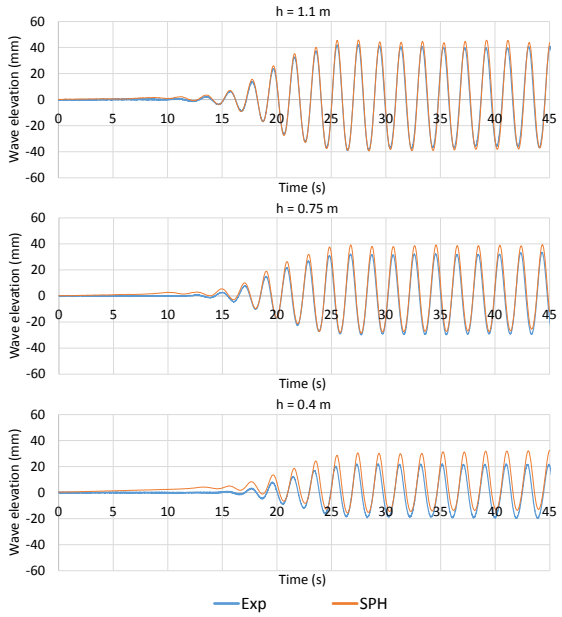

Fig.6 Comparison of wave elevation between experiment and SPH with A= 33.0 mm and T =1.95 s

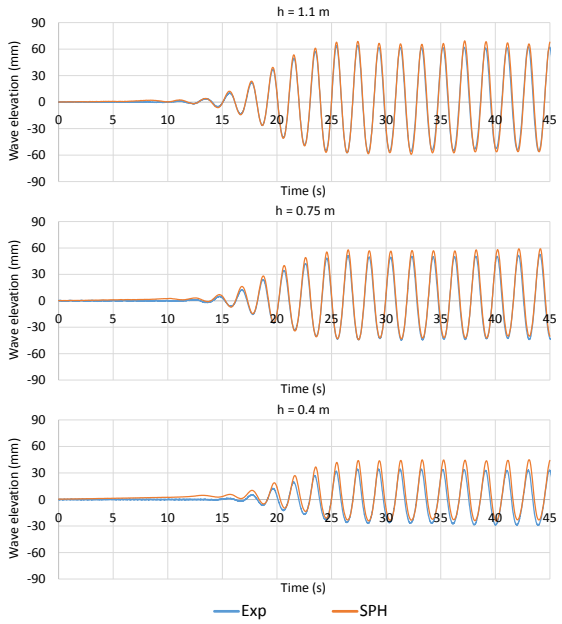

Fig.7 Comparison of wave elevation between experiment and SPH with A= 50.5 mm and T =1.95 s

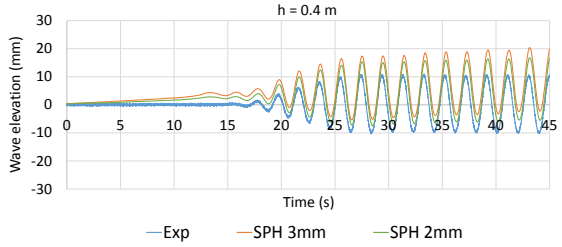

Fig.8 Influence of particle size on wave amplitude and average shift

Figs.9-11 are comparison results of wave elevation at T=1.15 s. The SPH simulations show quantitative agreement with the experiment in deep and shallow waters. Nonlinear asymmetric water waves are well reproduced by SPH for with A=50.5 mm. Especially for h=0.4 m, wave profile is different from sinusoidal wave in the experiment and this steep shallow water waves can be well predicted by SPH as presented in Fig.12. at t=38.2 s and t=38.8 s. Table 5 shows the average of steady wave amplitude in steady state in the experimental and numerical results as well as a first-order wave maker theory known as Biesel transfer function (Biésel and Suquet, 1951) given in Eq.8. The maximum error of SPH is found for T=1.95 s, A=33.0 mm and h=0.4 m, but it is less than 10 % and average error is 6.0 % though the measurement point is far from the wave maker. The Biesel transfer function gives maximum error of 32 % and average error is 11.7 %.

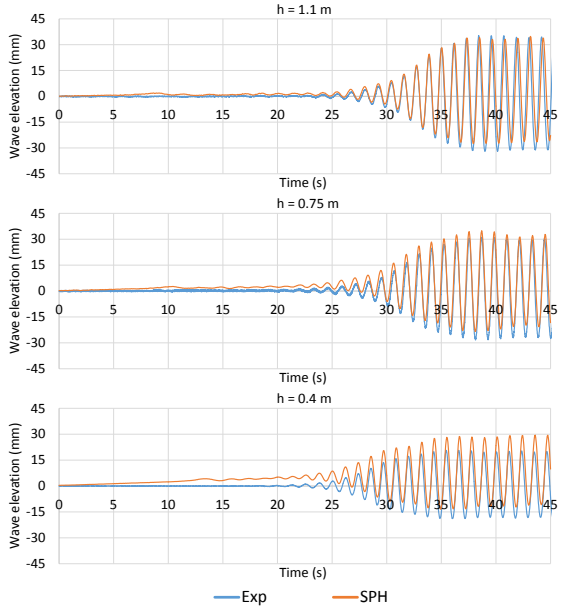

Fig.9 Comparison of wave elevation between experiment and SPH with A=16.5 mm and T =1.15 s

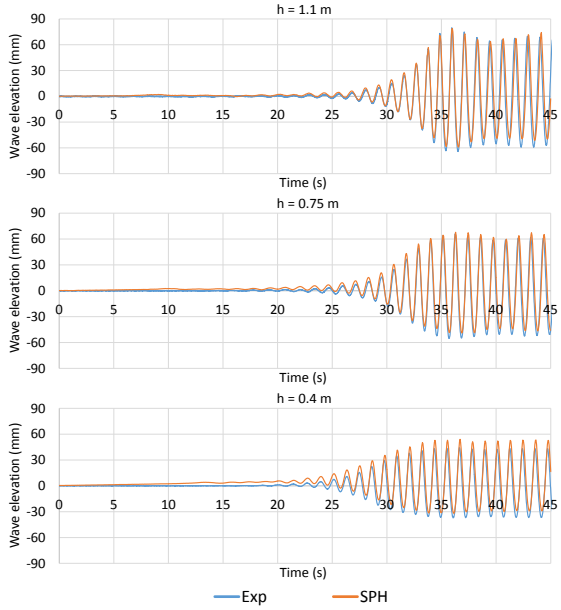

Fig.10 Comparison of wave elevation between experiment and SPH with A=33.0 mm and T =1.15 s

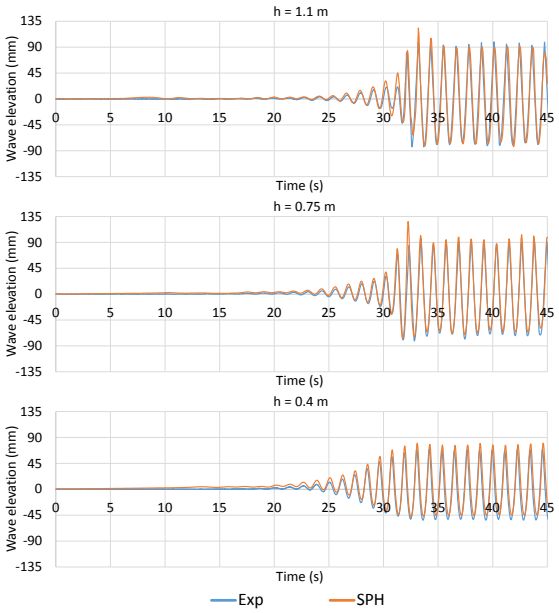

Fig.11 Comparison of wave elevation between experiment and SPH with A=50.5 mm and T =1.15 s

Table 5 Results of steady wave amplitude

T (s)	A (mm)	h (m)	Exp. (mm)	SPH (mm)	Error (%)	Biesel T.F. (mm)	Error (%)
1.95	16.5	1.1	18.2	19.6	7.7	18.6	2.2
		0.75	14.9	15.7	5.4	13.0	-12.8
		0.4	10.3	11.1	7.8	7.0	**-32.0**
	33.0	1.1	38.5	41.4	7.5	37.3	-3.1
		0.75	30.8	32.9	6.8	26.0	-15.6
		0.4	20.5	22.5	**9.9**	14.0	-31.7
	50.5	1.1	57.9	61.7	6.6	57.0	-1.6
		0.75	46.8	49.7	6.2	39.8	-15.0
		0.4	30.7	33.7	9.8	21.4	-30.3
1.15	16.5	1.1	32.9	30.1	-8.5	32.4	-1.5
		0.75	26.8	28.7	7.1	29.5	10.1
		0.4	20.4	19.1	-6.4	19.4	-4.9
	33.0	1.1	62.3	58.0	-6.9	64.8	4.0
		0.75	53.2	55.5	4.3	59.0	10.9
		0.4	40.6	39.6	-2.5	38.7	-4.7
	50.5	1.1	83.9	86.8	3.5	99.1	18.1
		0.75	81.7	81.0	-0.9	90.4	10.6
		0.4	60.6	60.0	-1.0	59.3	-2.1

$$\frac{H}{2}=\frac{2\sinh^2\left(\frac{2\pi h}{\lambda}\right)}{\frac{2\pi h}{\lambda}+\sinh\left(\frac{2\pi h}{\lambda}\right)\cosh\left(\frac{2\pi h}{\lambda}\right)}A \quad (8)$$

The time history of wave elevation is well predicted by SPH. However it is validated at one particular distance from the wave maker. For comprehensive validation, it is needed to check the wave decay rate along the propagation distance. Therefore the steady amplitudes at different distance from the wave maker are compared between experiment and simulation as in Fig.13. The wave amplitude decreases slightly with travel distance in the experiment and the SPH result shows quite similar decay rate for both wave periods. This result suggests the energy conservation is well achieved and the energy dissipation due to friction with tank bottom is represented in the SPH model.

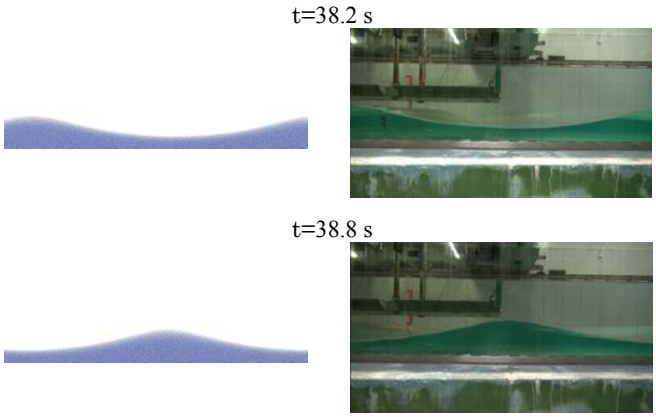

Fig.12 Comparison of wave surface profile with h=0.4 m, A=50.5 mm and T=1.15 s

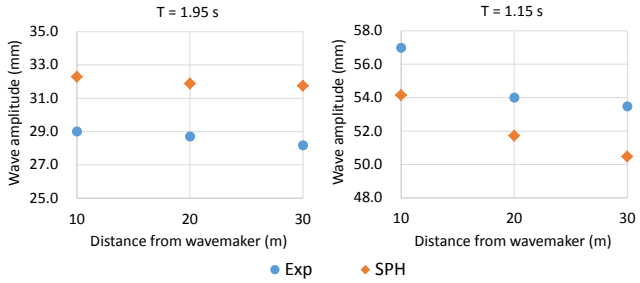

Fig.13 Comparison of decay of wave amplitude between experiment and SPH

Wave pressure

Prior to the discussion on dynamic wave pressure, verification of the SPH model for hydrostatic pressure is needed. The hydrostatic pressure at the tank bottom with water depth of 1.1 m is calculated without the movement of wave maker. The analytical and SPH results are 10.5 kPa and 10.7 kPa respectively and the error is 1.87%, and smooth pressure gradient is obtained as presented in Fig.14.

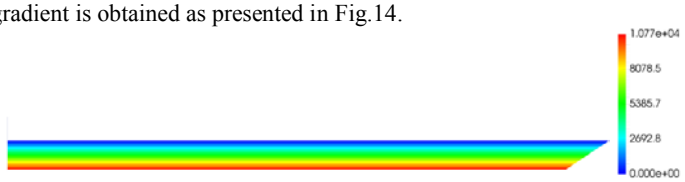

Fig.14 Contour of hydrostatic pressure with h=1.1 m

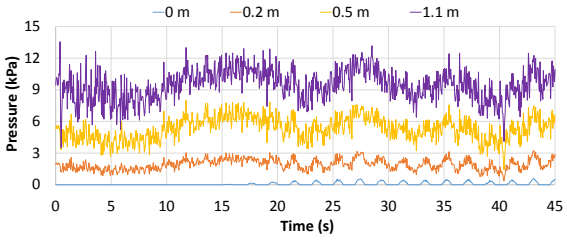

Fig.15 Pressure variation of SPH at different depths with h=1.1 m and A=50.5 mm

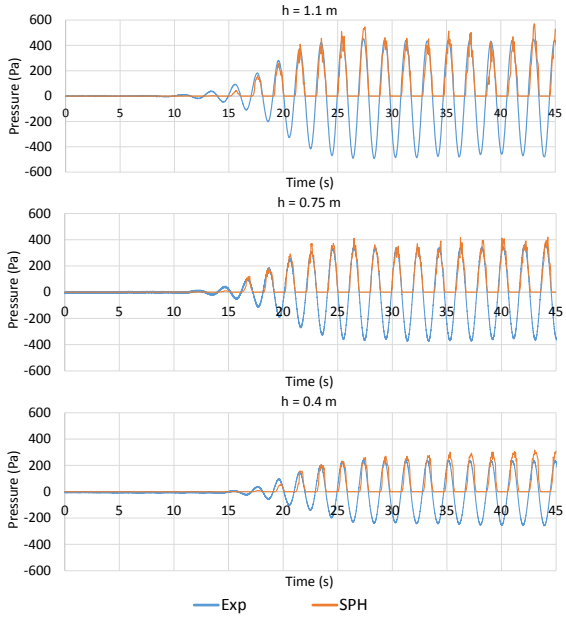

Fig.16 Comparison of wave pressure between experiment and SPH with A= 50.5 mm and T =1.95 s

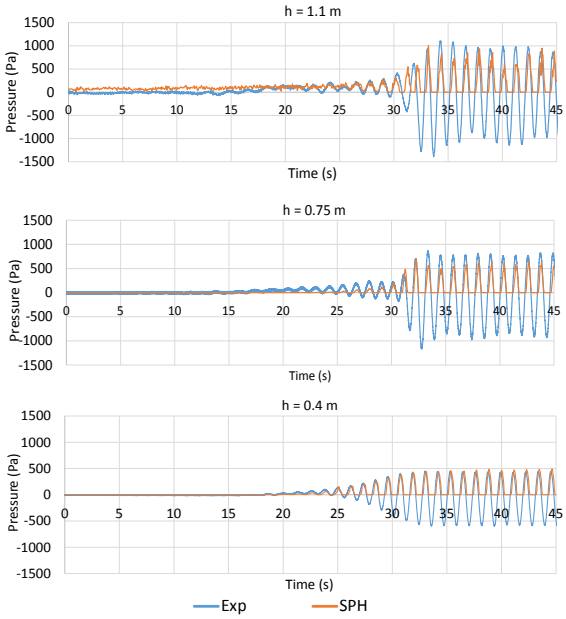

Fig.17 Comparison of wave pressure between experiment and SPH with A=50.5 mm and T =1.15 s

Fig.15 shows calculated pressure variation at several depths. Here depths of 1.1 m and 0 m mean the pressure is detected on the tank bottom and on the calm-water surface. Unfavorable pressure fluctuation with wide frequencies appears at depth of 1.1 m, but it decreases as the detection position closes to the wave surface. Figs.16-17 show comparison results of wave pressure with the maximum piston motion. Here the experimental result is converted from the bottom to the calm-water surface by multiplying $\cosh(2\pi h/\lambda)$ with the measured pressure, based on linear wave theory. Wave pressure is calculated at the fixed point on the original still water surface, so negative pressure cannot be detected in SPH results. The numerical fluctuation does not appear and the dynamic wave pressure is nicely predicted for all tested conditions. In case with largest water depth at T=1.15 s, pressure strongly oscillates periodically from the beginning. This could be presumed as internal pressure wave because wave elevation is not confirmed in Fig.11. SPH cannot reproduce this pressure wave with tested numerical parameters.

Wave deformation due to obstacle

The SPH model shows high capability to generation and propagation of nonlinear water waves. Then we try to confirm applicability of SPH to large deformation of water waves due to sudden change of water depth. For this purpose, we conduct a wave generation test with a box-shape obstacle (0.5 m in length, 5.25 m in width, and 0.4 m in height) with h=0.6 m, A=50.5 mm and T=1.15 s. Comparison of wave elevation at the center of box and wave surface deformation are shown in Fig. 18 and 19, respectively. In the time history, the wave elevation becomes asymmetric in vertical direction because the shape of wave crest is sharpened due to significant reduction of water depth, then finally wave is breaking behind the box. The SPH result captures this nonlinear deformation of wave surface in good accuracy.

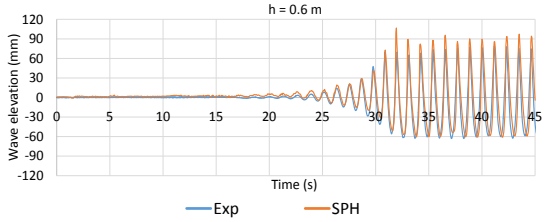

Fig.18 Comparison of water elevation between experiment and SPH with obstacle with A=50.5 mm and h=0.6 m

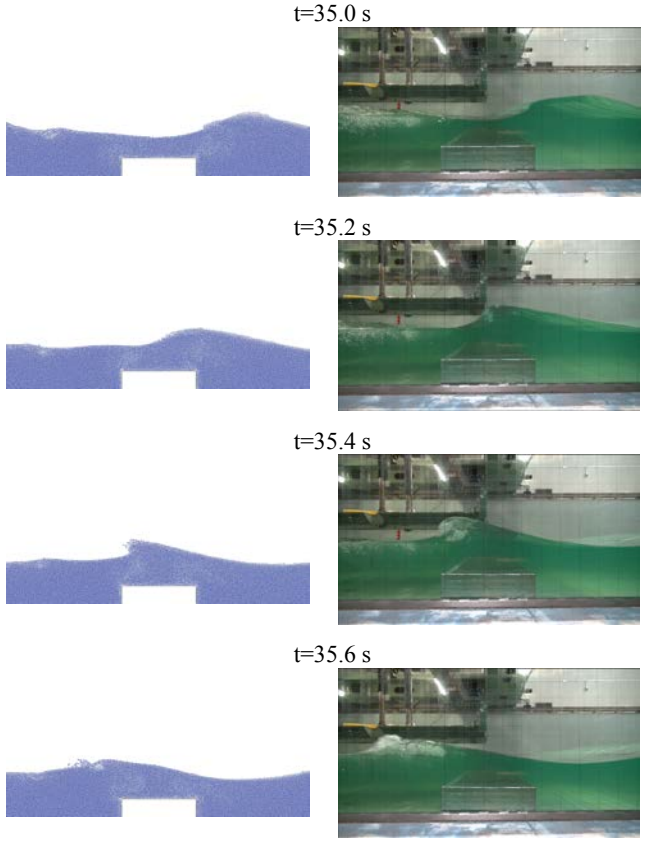

Fig.19 Comparison of wave surface deformation due to existence of obstacle with h=0.6 m

CONCLUSIONS

We conducted experimental validation of SPH model for the wave generation and propagation in both deep and shallow waters. The SPH simulation, which directly uses the measured piston motions of wave-making board, shows quantitative agreement with the dedicated experimental data in terms of the wave amplitude, wave surface profile, phase velocity and wave decay rate in its propagation, when the number of particles especially in vertical direction is appropriately set in consideration of the wave amplitude and water depth. Dynamic wave pressures are also well reproduced near the water surface but the numerical pressure oscillations cannot be avoided when the gauging point becomes relatively deeper. The SPH computations can also capture the nonlinear large deformation of wave surface, including its breaking, due to the rapid change of water depth arising from the existence of an obstacle. Through a series of robust validations of SPH in this paper, the validity of SPH for wave generation and propagation is clearly demonstrated. Therefore we can apply the SPH model to advanced engineering applications as a potential tool.
The authors are willing to provide the experimental data for benchmark study in the international research community.

ACKNOWLEDGEMENTS

The first author wishes to thank the Directorate General of Resources for Science, Technology and Higher Education, Ministry of Research, Technology and Higher Education of Indonesia a sponsor of the first author for study at Kobe University.

REFERENCES

Altomare, C., Crespo, A.J.C., Rogers, B.D., Dominguez, J.M., Gironella, X., and Gómez-Gesteira, M. (2014). Numerical modelling of armour block sea breakwater with smoothed particle hydrodynamics, *Computers & Structures*, *130*, 34–45.

Antuono, M., Colagrossi, A., Marrone, S., Lugni, C. (2011). Propagation of gravity waves through an SPH scheme with numerical diffusive terms, *Computer Physics Communications, 182*, 866-877.

Barreiro, A., Crespo, A.J.C., Domínguez, J.M., Gómez-Gesteira, M. (2013), Smoothed Particle Hydrodynamics for coastal engineering problems, *Computers and Structures, 120*, 96-106.

Biésel, F., and Suquet, F. (1951). Les appareils générateurs de houle en laboratoire - Laboratory wave generating apparatus, *La Houille Blanche*, *6*(2), 147–165.

Crespo, A.J.C., Domínguez, J.M., Rogers, B.D., Gómez-Gesteira, M., Longshaw, S., Canelas, R., and García-Feal, O. (2015). DualSPHysics: Open-source parallel CFD solver based on Smoothed Particle Hydrodynamics (SPH), *Computer Physics Communications*, *187*, 204–216.

Gingold and Monaghan, J. J. (1977). Smoothed Particle Hydrodynamics: Theory and Application to Non-Spherical Stars, *Mon.Not.R.ast.Soc*, *181*, 375–389.

Gotoh, H., Shao, S.D, and Memita T (2004). SPH-LES Model For Numerical Investigation Of Wave Interaction With Partially Immersed Breakwater, *Coastal Engineering Journal*, *46*, 39–63.

Kawamura, K., Hashimoto, H., Matsuda, A., and Terada, D. (2016). SPH simulation of ship behaviour in severe water-shipping situations, *Ocean Engineering*, *120*, 220-229.

Le Touzé, D., Marsh, A., Oger, G., Guilcher, P. M., Khaddaj-Mallat, C. (2010). Alessandrini, B. and Ferrant, P., SPH simulation of green water and ship flooding scenarios, *Journal of Hydrodynamics, Ser. B*, *22*, 231–236.

Marrone, S., Autuono, M., Golagrossi, A., Colicchio, G., Le Touzé, D., Graziani G. (2011) δ-SPH model for simulating violent impact flows, *Computer Methods in Applied Mechanics and Engineering, 200, 13-16*, 1526-1542.

Molteni, D., Colagrossi, A. (2009). A simple procedure to improve the pressure evaluation in hydrodynamic context using the SPH, *Computer Physics Communications, 180*, 861-872.

Monaghan, J.J. (1992). Smoothed Particle Hydrodynamics, *Annual Review of Astronomy and Astrophysics*, *30*, 543–74.

Monaghan, J.J. (1994). Simulating Free Surface Flows with SPH, *Journal of Computational Physics*, *110*, 399–406.

Shao, S.D. (2005). SPH Simulation Of Solitary Wave Interaction With A Curtain-Type Breakwater, *Journal of Hydraulic Research*, *43*, 366–375.

Skillen, A., Lind, S., Stansby, P.K., Rogers, B.D., (2013). Incompressible Smoothed Particle Hydrodynamics (SPH) With Reduced Temporal Noise And Generalised Fickian Smoothing Applied to Body–Water Slam And Efficient Wave–Body Interaction, *Comput. Methods Appl. Mech. Engrg*, *265*, 163–173.